Systems/Circuits

Gain Modulation of Synaptic Inputs by Network State in Auditory Cortex *In Vivo*

Ramon Reig,[1] Yann Zerlaut,[2] Ramiro Vergara,[1] Alain Destexhe,[2] and Maria V. Sanchez-Vives[1,3]

[1]Institut d'Investigacions Biomèdiques August Pi i Sunyer, 08036 Barcelona, Spain, [2]Unité de Neurosciences, Information et Complexité, CNRS, 91198 Gif sur Yvette, France, and [3]Institució Catalana de Recerca i Estudis Avançats, 08010 Barcelona, Spain

The cortical network recurrent circuitry generates spontaneous activity organized into Up (active) and Down (quiescent) states during slow-wave sleep or anesthesia. These different states of cortical activation gain modulate synaptic transmission. However, the reported modulation that Up states impose on synaptic inputs is disparate in the literature, including both increases and decreases of responsiveness. Here, we tested the hypothesis that such disparate observations may depend on the intensity of the stimulation. By means of intracellular recordings, we studied synaptic transmission during Up and Down states in rat auditory cortex *in vivo*. Synaptic potentials were evoked either by auditory or electrical (thalamocortical, intracortical) stimulation while randomly varying the intensity of the stimulus. Synaptic potentials evoked by the same stimulus intensity were compared in Up/Down states. Up states had a scaling effect on the stimulus-evoked synaptic responses: the amplitude of weaker responses was potentiated whereas that of larger responses was maintained or decreased with respect to the amplitude during Down states. We used a computational model to explore the potential mechanisms explaining this nontrivial stimulus–response relationship. During Up/Down states, there is different excitability in the network and the neuronal conductance varies. We demonstrate that the competition between presynaptic recruitment and the changing conductance might be the central mechanism explaining the experimentally observed stimulus–response relationships. We conclude that the effect that cortical network activation has on synaptic transmission is not constant but contingent on the strength of the stimulation, with a larger modulation for stimuli involving both thalamic and cortical networks.

Key words: cerebral cortex; computational model; oscillations; synaptic inputs; thalamocortical; Up states

Introduction

Cortical spontaneous activity varies with the brain's functional state. During slow-wave sleep and anesthesia, this activity is organized in slow oscillations (Steriade et al., 1993) generated through the recurrent connectivity between cortical neurons (Lorente de Nó, 1938). These slow oscillations are characterized by active periods of high synaptic activity, depolarized membrane potential, and neuronal firing (Up states) interspersed with silent periods of low synaptic activity and hyperpolarized membrane potential or Down states (Metherate and Ashe, 1993; Steriade et al., 1993; Cowan and Wilson, 1994; Sanchez-Vives and McCormick, 2000; Petersen et al., 2003). Network activity has an impact on different properties of the network itself, including intrinsic

(Paré et al., 1998; Steriade, 2001) and circuit properties (Boudreau and Ferster, 2005; Crochet et al., 2005; Crochet et al., 2006; Reig et al., 2006; Haider et al., 2007; Reig and Sanchez-Vives, 2007). One of these network properties is synaptic responsiveness. Different studies have analyzed how cortical states affect synaptic responsiveness (Timofeev et al., 1996) and sensory transmission (Azouz and Gray, 1999; Petersen et al., 2003; Sachdev et al., 2004; Crochet et al., 2005; Crochet et al., 2006; Haider et al., 2007; Hasenstaub et al., 2007; Reig and Sanchez-Vives, 2007; Rigas and Castro-Alamancos, 2009), yielding diverse and sometimes contradictory results. Depending on the cortical areas and on the protocols used, Up states have been reported either to decrease (Petersen et al., 2003; Sachdev et al., 2004; Crochet et al., 2006; Hasenstaub et al., 2007; Rigas and Castro-Alamancos, 2009) or to increase (Azouz and Gray, 1999; Haider et al., 2007; Reig and Sanchez-Vives, 2007) cortical responsiveness with respect to Down states.

Understanding gain modulation during Up states is also important because cortical dynamics during wakefulness shares properties with Up states (Steriade et al., 2001; Destexhe et al., 2007; Constantinople and Bruno, 2011). Computational models suggest that several features of Up states may provide interesting computational properties such as making neurons probabilistic and thus controlling their gain and transfer function (Hô and Destexhe, 2000; Destexhe and Contreras, 2006). It is therefore of primary importance to understand such interactions.

To understand quantitatively the neuronal transfer function during Up states, we recorded intracellularly from A1 (auditory cortex) neurons *in vivo* synaptic potentials evoked by either auditory or electrical stimulation (intracortical or thalamocortical) over a wide range of intensities. The activation of cortical neuronal populations by auditory stimuli and during spontaneous activity under anesthesia has been described previously (Luczak et al., 2009; Sakata and Harris, 2009). However, the extent to which cortical activation imposes a modulation of synaptic inputs depending on the intensity of the stimulus has not been reported. We find that Up states can gain-modulate synaptic responses by either enhancing or decreasing synaptic potentials contingent on the intensity of stimulation. The result is a global scaling of the evoked responses. To understand the network mechanisms mediating this stimulus–response relationship, we modeled different ensembles of the full recurrent and feedforward sensory pathway to account for the auditory, intracortical, and thalamocortical stimulation. We provide a quantitative mechanism that produces the gain modulation of synaptic responses during Up states.

Materials and Methods

Ethics approval

The experiments described here have been approved by the Animal Ethics Committee of the University of Barcelona under the supervision of the Autonomous Government of Catalonia and following the guidelines of the European Communities Council (86/609/EEC).

Intracellular recordings from rat auditory cortex

Adult male Wistar rats (200–340 g; $n = 29$) were used for recordings in auditory cortex (A1). Anesthesia was induced by injection of ketamine (80 mg/kg) and xylazine (8 mg/kg). Anesthesia levels were monitored by the heart rate (240–300 bpm), blood O_2 concentration (95%), the recording of low-frequency electroencephalogram, and the absence of reflexes. The animals were not paralyzed. The maintenance dose of ketamine was 30–50 mg/kg/h and xylazine 1–2 mg/kg/h. Intraperitoneal maintenance doses of anesthesia were given with intervals of 30–70 min and an overdose was given at the end of the experiment. Rectal temperature was maintained at 37°C during the experiment. Once in the stereotaxic apparatus, a craniotomy (2 × 2 mm) was made at coordinates AP −4.30 from bregma, L 7 mm (Paxinos and Watson, 2005). After opening the dura, intracellular recordings were obtained with borosilicate glass capillaries 1 mm outer diameter × 0.5 inner diameter (Harvard Apparatus). For stability and to avoid desiccation agar (4%) was used to cover the area.

Sharp intracellular recording electrodes were formed on a Sutter Instruments P-97 micropipette puller from medium-walled glass and beveled to final resistances of 50–100 MΩ. Micropipettes were filled with 2 M potassium acetate. Only very stable recordings were included (average duration 58 min) and they all had overshooting action potentials and a stable input resistance. Recordings were digitized, acquired, and analyzed using a data acquisition interface and software from Cambridge Electronic Design and its commercial software Spike 2. Further details of the procedure can be found in Reig and Sanchez-Vives (2007).

Conductance measurement

By means of intracellular injection of DC current, the membrane potential of auditory neurons was current clamped at different membrane potentials as in Compte et al. (2009). The bridge was carefully balanced at each DC level to compensate for the electrode resistance. The distribution of subthreshold membrane potential values was obtained for each membrane potential level, yielding a bimodal distribution corresponding to Up and Down states (Fig. 1D). An I–V relationship between the Up and Down state peak values of the bimodal distribution and the value of the DC-injected current was built, the inverse of the slope being the conductance.

Electrical stimulation

Electrical stimulation (0.2 ms, 10–300 μA) was delivered by means of a WPI A-360 stimulus isolation unit that prevents electrode polarization.

Thalamocortical (TC) or intracortical (IC) fibers were stimulated with bipolar electrodes made of sharpened tungsten wires. The stimulation electrode was placed in the medial geniculate nucleus of the thalamus (−5.6 mm AP, −3.4 mm L, 5.2–6.2 mm D). To ensure that the location was correct, first, the electrode was used to record thalamic responses to auditory stimulation and then it was switched to the stimulation mode. Thalamocortical electrical stimulation evoked onset postsynaptic potentials with latencies ranging between 2.3 and 5 ms. Intracortical electrical stimulation was delivered by means of a bipolar electrode in the vicinity of the intracellularly recorded neuron (0.5–1.5 mm as in Reig et al., 2006). This stimulation evoked postsynaptic potentials with latencies ranging between 1.7 and 3.5 ms.

In the series of electrical stimulation, for each one of the intensities, a minimum of 100 shocks were given at 0.2–0.33 Hz. The stimulation could randomly occur during Up or Down states and were sorted out during the offline analysis.

Auditory stimulation

A click of white noise of 5 ms of duration was used to stimulate. White noise was generated by a MATLAB sequencer and recorded with the data acquisition system. Stimuli onset and duration were controlled by a computer. The stereotaxic frame had hollow ear bars and the loudspeakers were placed inside them (Sanchez-Vives et al., 2006). Therefore, stimuli were delivered binaurally through a closed acoustic system based on Sony MDR E-868 earphones housed in a metal enclosure and surrounded by damping material that fit into the Perspex specula (Rees et al., 1997). The output of the system for each stimulus was calibrated to be between 55 and 85 dB$_{SPL}$. We used a series of 90–100 clicks at 0.2–0.33 Hz for each intensity value, the stimulus occurring on different phases of the oscillatory cycle. The analysis was done offline and the synaptic responses were sorted for different periods of the cycle (Up states, Down states, etc).

Detection of Up and Down states

Up and Down states were detected using an algorithm described in Seamari et al. (2007). This algorithm calculates the two exponential moving averages of the membrane potential, a slow and a fast one. The size of the windows for averaging are calculated for each particular signal and the system uses the information of the previous dynamics of the system to predict the future transitions. The crossing of the slow and fast moving averages provides a good estimation of the Up/Down states transitions. A more precise method is also integrated to better determine the moment of Up/Down transition based on the momentum. These two combined methods are reliable and work better than other detection methods even in noisy conditions (Seamari et al., 2007). The classification of responses was done following Reig and Sanchez-Vives (2007) into those occurring during Up and during Down states. This classification of responses was checked on a single response basis by hand.

Analysis

The amplitude of the postsynaptic potentials (PSPs) was measured at the peak, which had latencies between 4 and 10 ms. PSP slope and amplitude were highly correlated (Reig et al., 2006). When normalization was necessary to compare synaptic potentials evoked in Up versus Down states, it was done with respect to the amplitude of the PSPs during Down states. Next, the normalized values for individual neurons were averaged to provide population data; these values were depicted in the scatter diagrams in the different figures. Absolute values are also provided. Data are given in the text as mean ± SD. Error bars in the figures correspond to the SEM.

Model

In this section, we propose a quantitative description of how the cell and network properties during Up and Down states shape the postsynaptic response to a given stimulation. Two cases are considered, intracortical and thalamocortical stimulation. We performed this study using analytical approximations of the different processes.

The general strategy that we adopt is related to the probabilistic theoretical framework that was described previously (Hô and Destexhe, 2000; Destexhe and Contreras, 2006).

The information needed to derive the effect of the stimulus on a network is as follows. At the cellular level, we need to know the relationship

Table 1. Parameters of the model

Name	Symbol	Value
Cellular properties		
Leak conductance	g_L	10 nS
Membrane capacitance	C_m	200 pF
Leak reversal potential	E_L	−65 mV
Threshold potential	V_{thre}	−50 mV
Refractory period	τ_{ref}	5 ms
Synapses		
Excitatory cortical weight	$Q_{e,cort}$	0.4 nS
Inhibitory cortical weight	$Q_{i,cort}$	1.2 nS
Excitatory thalamic weight	$Q_{e,thal}$	2 nS
Excitatory time constant	τ_e	7.3 ms
Inhibitory time constant	τ_i	5 ms
Excitatory reversal potential	E_e	0 mV
Inhibitory reversal potential	E_i	−80 mV
Background activity: cortical network		
Mean excitatory conductance: Up state	$\bar{g}_e^{Up}$	7 nS
Mean inhibitory conductance: Up state	$\bar{g}_i^{Up}$	20 nS
Standard deviation excitatory conductance: Up state	σ_e^{Up}	3 nS
Standard deviation inhibitory conductance: Up state	σ_i^{Up}	8 nS
Mean excitatory conductance: Down state	$\bar{g}_e^{Down}$	1 nS
Mean inhibitory conductance: Down state	$\bar{g}_i^{Down}$	2 nS
Standard deviation excitatory conductance: Down state	σ_e^{Down}	0.1 nS
Standard deviation inhibitory conductance: Down state	σ_i^{Down}	0.5 nS
Background activity: thalamic network		
Mean membrane potential: Up state	$\mu_{V,thal}^{Up}$	−61 mV
Standard deviation membrane potential: Up state	$\sigma_{V,thal}^{Up}$	5 mV
Mean membrane potential: Down state	$\mu_{V,thal}^{Down}$	−64 mV
Standard deviation membrane potential: Down state	$\sigma_{V,thal}^{Down}$	4 mV
Network architecture		
Cortical recurrent connectivity probability	ε_{cort}	2%
Thalamocortical afference probability	ε_{thal}	2%
Number of cells: cortical network	N_{cort}	10000
Percentage of cortical inhibitory neurons	g	25%
Number of excitatory cells: thalamic network	N_{thal}	2000
Electrical stimulation model		
Cortical maximal radius	$r_{\mathrm{max},cort}$	1 mm
Cortical minimal radius	$r_{0,cort}$	300 μm
Depolarization relation: cortical stimulation	$\Delta V_{cort}(I, r)$	$0.6 \cdot \dfrac{I}{1 + \left(\dfrac{r}{r_{0,cort}}\right)^2} - 1$
Thalamic maximal radius	$r_{\mathrm{max},thal}$	200 μm
Thalamic minimal radius	$r_{0,thal}$	60 μm
Depolarization relation: thalamic stimulation	$\Delta V_{thal}(I, r)$	$0.056 \cdot \dfrac{I + 316.2}{1 + \left(\dfrac{r}{r_{0,thal}}\right)^2} - 315.3$

between the input intensity and the firing probability, this is the "activation function." A given stimulus has a differential effect over cells within the network (e.g., in the case of an electrical stimulation, the distance to the electrode or in the case of an afferent network the wiring realizations to the different cells), so we will compute the histogram over cells of the effect of this stimulus. We will finally apply the "activation function" on the histogram of the stimulus effect to get the number of spiking cells and then derive the postsynaptic response.

Cell properties. We use the Leaky Integrate and Fire model (later adapted from Lapicque (1907)) to describe the neurons. For simplicity, the three populations considered here (excitatory cortical neurons, inhibitory cortical neurons, and thalamocortical neurons) have identical properties and the parameters can be found in Table 1.

The subthreshold dynamics results from passive and synaptic currents. The passive properties are described by a simple RC circuit, the capacitive current is characterized by a membrane capacitance C_m, the leak current is set by a conductance g_L and a reversal potential E_L. The membrane equation below threshold is therefore:

$$C_m \frac{dV}{dt} = g_L (E_L - V) + I_{syn}(V, t) \qquad (1)$$

The synaptic currents $I_{syn}(V, t)$ integrate excitatory and inhibitory input with reversal potentials E_e and E_i. Their respective conductances, G_e and G_i, will be determined by the sum of the background and stimulus-evoked activity. The synaptic current is given by:

$$I_{syn}(V, t) = G_e(t) \cdot (E_e - V) + G_i(t) \cdot (E_i - V) \qquad (2)$$

The spiking mechanism is described by a simple threshold crossing: we consider that a spike is emitted when $V(t)$ reaches the threshold membrane potential value V_{thre} and from that moment the neuron is at rest during a period τ_{ref} before the subthreshold dynamics can restart.

Architecture of the network models. The cortical network is modeled as a random recurrent network of $N_{cort} = 10000$ cells, where $g = 25\%$ are inhibitory neurons and with a probability of connection $\varepsilon_{cort} = 2\%$. In the thalamic network, we consider only the $N_{thal} = 2000$ excitatory thalamocortical cells that project onto the cortical network with a connection probability $\varepsilon_{thal} = 2\%$.

Background cortical activity. The cortical network activity is made of excitatory and inhibitory recurrent input and we describe this background input as Ornstein-Uhlenbeck processes. So, in general:

$$dG_{syn}^{bg} = (\overline{g_{syn}} - G_{syn}^{bg}) \cdot \frac{dt}{\tau_{syn}} + \sqrt{2\tau_{syn}}\sigma_{syn} \cdot dW \quad (3)$$

where dW is a Wiener process and $syn \in \{e, i\}$ is the index for the excitation and the inhibition, respectively.

This input varies considerably between Up and Down states. The Up state is characterized by a very high synaptic bombardment, whereas the synaptic activity is almost null in the Down state. This can be seen in the values of Table 1. The autocorrelation time τ_{syn} is taken as the same as the synaptic decay time in the explicit model of synaptic conductance time course.

The membrane potential fluctuations resulting from this input have been studied analytically (Richardson, 2004; Rudolph and Destexhe, 2005) and we use the Gaussian approximation formulated in Rudolph et al. (2004) for the stationary membrane potential distribution $\rho^s(V)$ as follows:

$$\rho^S(V) = \frac{1}{\sigma_V^S \sqrt{2\pi}} e^{\frac{-(V-\mu_V^S)^2}{\sqrt{2}\sigma_V^S}} \quad (4)$$

With the mean μ_V^S, standard deviation σ_V^S, and effective membrane time constant τ_m^S given by the following:

$$\begin{cases} \mu_V^S = \frac{\bar{g}_e^S E_e + \bar{g}_i^S E_i + g_L E_L}{\bar{g}_e^S + \bar{g}_i^S + g_L} \\ \tau_m^S = \frac{C_m}{\bar{g}_e^S + \bar{g}_i^S + g_L} \\ (\sigma_V^S)^2 = \left(\frac{\sigma_e^S \tau_m^S}{C_m}\right)^2 \frac{\tau_e}{\tau_m^S + \tau_e}(\mu_V^S - E_e)^2 + \left(\frac{\sigma_i^S \tau_m^S}{C_m}\right)^2 \frac{\tau_i}{\tau_m^S + \tau_i}(\mu_V^S - E_i)^2 \end{cases} \quad (5)$$

Here, S indexes the dependency of the network state, either Up or Down.

Background thalamic activity. We do not consider the effect of input within the thalamic network, so we do not explicitly describe the conductance state. The effect of the network state (Up or Down) will be described by a change of the Gaussian membrane potential distribution (Table 1); the mean and variance of the membrane potential are slightly increased in the Up state with respect to the Down state (Contreras et al., 1996).

Effect of the electrical stimulation. Our goal is to translate the electrical current injected through the bipolar stimulation into an histogram of depolarization across the considered network (cortical or thalamic). Modeling the complexity of such a phenomenon is not straightforward (Ranck, 1975), so we adopt an heuristic approach and derive simple expressions based on qualitative features. The parameters of those expressions are manually adjusted to bring the output of the model to approximate to the experimentally observed response in the Down state.

Our area of interest is the local network around the electrode, a network that is delimited by a crown of minimal radius (r_0) and maximal radius (r_{max}) of 0.3 and 1 mm, respectively, for the cortical network and 60 and 200 μm, respectively, for the thalamic network. The neuronal depolarization is linked to the intensity of the extracellular electric field (Ranck, 1975). Given the bipolar nature of the stimulation and the approximately isotropic resistive nature of gray matter (Logothetis et al., 2007), the electric field at $\vec{r}$ in the extracellular medium follows:

$$\vec{E}(\vec{r}) = \frac{I}{4\pi\sigma}((\vec{r} - \vec{r}_0)/\|\vec{r} - \vec{r}_0\|^3 - (\vec{r} + \vec{r}_0)/\|\vec{r} + \vec{r}_0\|^3) \quad (6)$$

Where σ is the extracellular conductivity, I is the injected current, $\vec{r}$ is the position in spherical coordinates, and the two electrodes are located in $\vec{r}_0$ and $-\vec{r}_0$.

This is a rather complicated expression and the final depolarization also depends on many factors, such as cellular orientation, myelination, and stimulus duration (Ranck, 1975). We do not need this level of detail—we only want to model the decaying impact of the stimulus within the local network of interest.

Therefore, from the previous expression, we will only keep the approximate quadratic decay of the modulus with distance (valid because we remain in a domain close enough from the stimulation electrode, between r_0 and r_{max}).

To this extracellular field, we associate a maximum depolarization value via an affine relation (the parameters of which are adjusted manually; Table 1). Our heuristic expression for the depolarization as a function of the injected current and distance from the electrode is then:

$$\Delta V(I, r) = \alpha \cdot \frac{I - \beta}{1 + (r/r_0)^2} - \gamma \quad (7)$$

To get the histogram of depolarization over the network, we need the radial density of neurons. Because of the laminar organization of the cells, we make the hypothesis of an homogenous surface density $D = \frac{N}{\pi \cdot (r_{max}^2 - r_0^2)}$, where N is the number of neurons within the network, we get a radial density:

$$N(r) = 2\pi \cdot r \cdot D \quad (8)$$

For a given current stimulation value, the depolarization– distance relation is monotonic (Equation 7) so we can easily apply the law of conservation of probability $dr \cdot N(r) = N_I(\Delta V) \cdot d\Delta V$ to calculate the histogram of depolarization $N_I(\Delta V)$ for an injected current I as follows:

$$N_I(\Delta V) = \frac{N \cdot r_0^2}{(r_{max}^2 - r_0^2)} \cdot \alpha \cdot \frac{I - \beta}{(\Delta V + \gamma)^2} \quad (9)$$

The quantity $N_I(\Delta V) \cdot d\Delta V$ represents the number of neurons in which the depolarization level lies between ΔV and $\Delta V + d\Delta V$ for a current input I. The few closest neurons will be maximally depolarized by $\Delta V(I, r_0)$ whereas the more numerous neurons at r_{max} will be depolarized by a much smaller quantity: $\Delta V(I, r_{max})$. Increasing the current level I shifts the histogram toward high depolarization. Examples for the shape of $N_I(\Delta V)$ can be seen in Figure 5B.

Recruitment of a stimulation within the neural network. Given a histogram of depolarization over the neural network (as provided by Equation 9), we wanted to estimate what fraction of the cells will fire as a response to this stimulus-evoked depolarization.

We consider a time bin of ~5 ms around the mean time of maximum depolarization induced by the stimulus. Within this time bin (as it is equal to the refractory period), the neurons can fire only once and we will split them between spiking and nonspiking. This temporal window is also lower than the membrane time constant (approximately 20 ms in the Down state and 5 ms in the Up state) so that the membrane potential fluctuations are weak within this window and we can classify the neurons according to their stationary membrane potential distribution $\rho^S(V)$ (as given by Equation 4 and 5). According to this classification, in the absence of stimulus, a fraction of neurons is firing due to background activity and the rest are silent. We then divide those silent neurons into two groups: the ones that the stimulus brings to fire and the ones that remain silent. The number of neurons that have a membrane potential above threshold (in the Up state in particular) is:

$$N_{bg} = N \cdot \int_{V_{thre}}^{\infty} \rho^S(V)dV = N_{tot}\left(1 - Erf\left(\frac{V_{thre} - \mu_V^S}{\sqrt{2} \cdot \sigma_V^S}\right)\right)/2, \text{ where}$$

N_{bg} corresponds to neurons that participate in the baseline firing rate and will induce the background (bg) conductance level in the next time bin. For those neurons, the stimulation will not affect their behavior within this time bin. We are interested in the evoked response that is due to the remaining neurons, those that would all be silent in the absence of stim-

ulation. In the absence of stimulation, their membrane potential follows the distribution:

$$\rho'^S(V) = \frac{\sqrt{2}}{\sqrt{\pi} \cdot \sigma_{VS} \cdot \left(1 + Erf\left(\frac{V_{thre} - \mu_V^S}{\sqrt{2} \cdot \sigma_V^S}\right)\right)} \cdot e^{-\left(\frac{V - \mu_V^S}{\sqrt{2} \cdot \sigma_V}\right)^2}$$

(10)

Within a time bin, they would take a random value from this distribution. So their probability to get above threshold in response to an evoked depolarization ΔV is given by:

$$f(\Delta V) = \int_{V_{thre} - \Delta V}^{V_{thre}} \rho'^S(V) \cdot dV$$

$$= \frac{Erf\left(\frac{V_{thre} - \mu_V^S}{\sqrt{2} \cdot \sigma_V^S}\right) - Erf\left(\frac{V_{thre} - \mu_V^S - \Delta V}{\sqrt{2} \cdot \sigma_V^S}\right)}{1 + Erf\left(\frac{V_{thre} - \mu_V^S}{\sqrt{2} \cdot \sigma_V^S}\right)}$$

(11)

We call this function the "activation function" of the network and it is an analytical analogous of the quantity introduced in the numerical study of Hô and Destexhe (2000). We use this quantity to calculate the number of activated neurons N_{act} as a result of a stimulation (synaptic or electrical) that produces the histogram of depolarization $N(\Delta V)$. This number is given by the following convolution:

$$N_{act} = \int_{\Delta V_{min}}^{\Delta V_{max}} f(\Delta V) \cdot N(\Delta V) \cdot d\Delta V$$

(12)

Where ΔV_{min} and ΔV_{max} are the minimum and maximum values of the stimulation, respectively.

Calculus of the PSP induced by the stimulus-evoked synaptic activity. On top of the stochastic background input, the cortical cells will be stimulated by the synaptic input resulting from the activity induced by the stimulation. We analyze how a deterministic synaptic input triggers a PSP response (as typically recorded in our experiments) depending on the network state. A synaptic event is modeled as a transient conductance change: an instantaneous jump of value Q_{syn} followed by an exponential decay of time constant τ_{syn} (the so-called "exponential synapse" model); $syn \in \{e, i\}$ is the index for the excitation and the inhibition, respectively.

For this calculation, we use the approximation presented in Kuhn et al. (2004), namely that the driving force is not modified within the time course of the response to the synaptic event. We consider that synaptic driving forces are constant $(E_{syn} - V(t)) \sim (E_{syn} - \mu_V^S)$ because they are fixed by the mean membrane potential μ_V^S. Therefore, we can rewrite Equation 1 as follows:

$$\tau_m^S \frac{dV}{dt} = \mu_V^S - V(t) + \frac{\tau_m^S}{C_m} \sum_{syn} \delta G_{syn}(t) \cdot (E_{syn} - \mu_V^S)$$

(13)

With this approximation, the effect of different synaptic events do not interact within each other (via the variation of the driving force) so that they sum independently. Therefore, we calculate the effect of one event and then sum linearly.

For one event starting at $t = 0$, the synaptic conductance variations will be $\delta G_{syn}(t) = Q_{syn}e^{-t/\tau_{syn}}H(t)$, so for $t \in [0, \infty]$, we get the membrane equation:

$$\tau_m^S \frac{dV}{dt} = \mu_V^S - V(t) + \frac{\tau_m^S}{C_m} \cdot (E_{syn} - \mu_V^S) \cdot Q_{syn} \cdot e^{-t/\tau_{syn}}$$

(14)

That has the following solution (given $V(0) = \mu_V^S$ and $\tau_m^S \neq \tau_{syn}$):

$$\begin{cases} V(t) = \mu_V^S + A_{syn} \cdot (e^{-t/\tau_m^S} - e^{-t/\tau_{syn}}) \\ A_{syn} = \frac{\tau_m^S \cdot Q_{syn} \cdot \tau_{syn}}{C_m \cdot (\tau_m^S - \tau_{syn})} \cdot (E_{syn} - \mu_V^S) \end{cases}$$

(15)

We next calculate the postsynaptic response in case of N_e and N_i excitatory and inhibitory events, respectively. For simplicity, all events arrive at the same time. The total membrane potential response is as follows:

$$V(t) = \mu_V^S + N_e \cdot A_e \cdot \left(e^{-t/\tau_m^S} - e^{-t/\tau_e}\right)$$

$$+ N_i \cdot A_i \cdot \left(e^{-t/\tau_m^S} - e^{-t/\tau_i}\right)$$

(16)

From this, we obtain that the time of maximum amplitude t_{max} is the solution of:

$$-\frac{(N_e \cdot A_e + N_i \cdot A_i) \cdot e^{-t_{max}/\tau_m^S}}{\tau_m^S} + \frac{N_e \cdot A_e \cdot e^{-t_{max}/\tau_e}}{\tau_e}$$

$$+ \frac{N_i \cdot A_i \cdot e^{-t_{max}/\tau_i}}{\tau_i} = 0$$

(17)

In practice, we will solve this using a Newton method and then compute the maximum amplitude response by evaluating $V(t_{max})$.

Results

Twenty-four intracellular recordings from primary auditory cortex in the ketamine/xylazine-anesthetized rat were included in the analysis (Fig. 1A). Neurons were classified into electrophysiological types following the method of Nowak et al. (2003). We identified 21 regular spiking (six of them "thin regular spiking"), one intrinsic bursting, and two fast-spiking neurons. The average input resistance was 28.7 ± 11.3 MΩ. Spontaneous and periodic Up states were interspersed with Down states generating an oscillatory rhythm (Fig. 1A,B), the intracellular potential showing the classical bimodal distribution (Fig. 1C; Steriade et al., 1993; Cowan and Wilson, 1994). The average duration of Up states was 0.43 ± 0.04 s and that of Down states 0.28 ± 0.02 s, resulting in an oscillatory frequency of 1.39 ± 0.11 Hz.

The conductance of six regular spiking neurons was estimated for both Up and Down states for different membrane potentials held by DC current injection (Paré et al., 1998; Waters and Helmchen, 2006). The bimodal distribution of membrane potential values at these different depolarization levels (Fig. 1D) was used to obtain the membrane potential values for Up and Down states and to construct the I–V relationships. In this way we estimated that the conductance (G) values were higher for Up than for Down states, with G_{Up}/G_{Down} of 2.5, 3.3, 2.7, 1.3, 2.2, and 2.6. Four of these examples are illustrated in Figure 1E.

The objective of the study was to determine how the occurrence of Up and Down states influenced the amplitude of synaptic potentials evoked by different intensities of stimulation—in other words, how the activity (Up states) or quiescence (Down states) in the cortical network influence synaptic transmission. With the purpose of analyzing the respective contributions to this modulation of the different blocks of the sensory pathway, synaptic potentials were evoked in three different ways: auditory stimulation (Fig. 2), electrical stimulation of intracortical connections (Fig. 3), and electrical stimulation of thalamocortical connections (Fig. 4).

Auditory stimulation

Auditory synaptic potentials were evoked by 5 ms clicks (see Materials and Methods) that were given every 3–5 s. The evoked
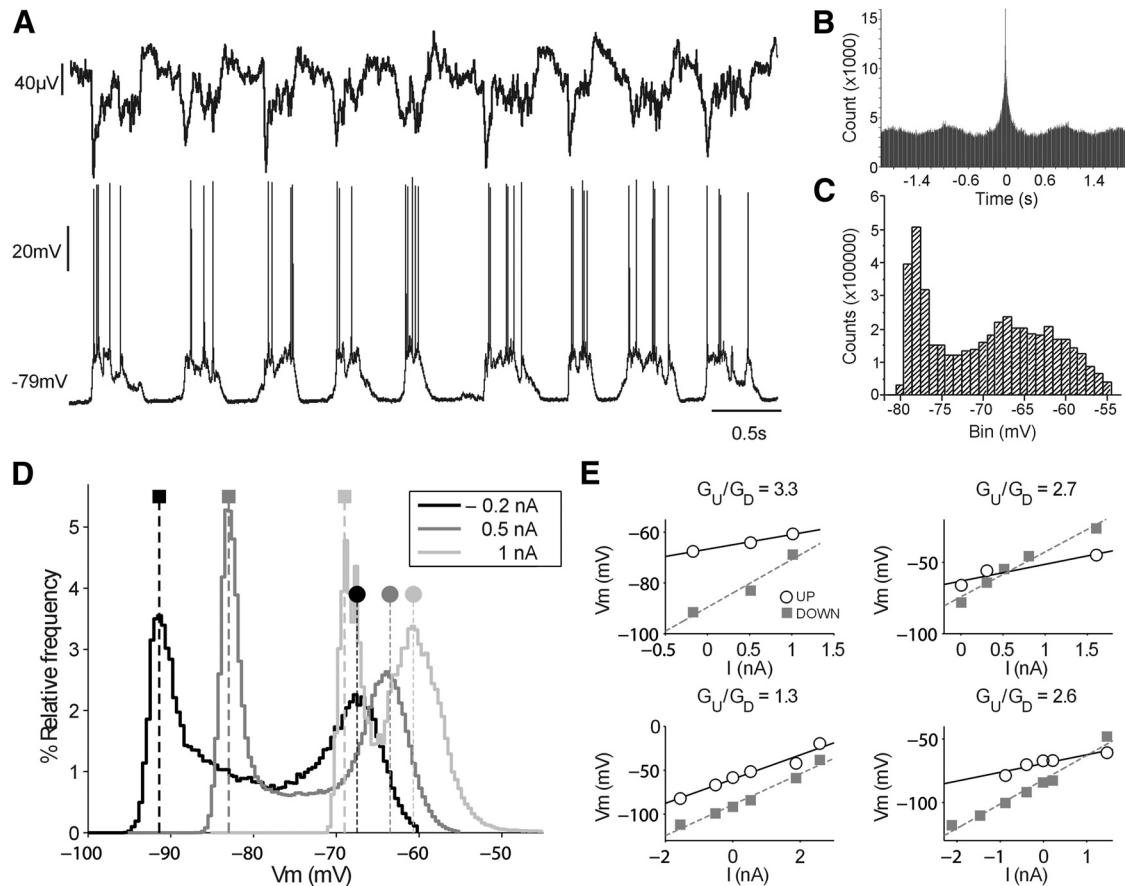
Figure 1. Slow oscillations in auditory cortex and auditory membrane conductances. **A**, Simultaneous LFP (top) and intracellular recording (bottom) of slow oscillations in A1. Note the neuronal firing during Up state and the decreased activity during Down state. **B**, Autocorrelogram of the neuronal firing illustrating the rhythmicity of the slow oscillations. **C**, Distribution of the membrane potential values resulting in the classical bimodal distribution that corresponds to Up (depolarized) and Down (hyperpolarized) states. Bin size = 1 mV. **D**, Distribution of the membrane potential values in one neuron for three different levels of DC current injection (grayscale for current). Notice that Up states (circles) had a larger overall conductance compared with Down states (squares). **E**, I–V plots for four different regular spiking neurons in A1. The inverse of the slope corresponds to the conductance (G) and G_{Up}/G_{Down} is indicated for each case on top of the I–V. Notice that, in all cases, the conductance is larger in the Up states.

auditory synaptic responses had an onset latency of 11.6 ± 2.2 ms and a peak latency of 21.8 ± 3.4 ms ($n = 9$ cells). Stimulus-evoked synaptic potentials occurred during Down or during Up states. Synaptic potentials occurring during Down states could also recruit the cortical network and thus evoke a new Up state. In those cases, the amplitude of the evoked synaptic potential is difficult to measure because the recruitment of the local network induces a further depolarization (Fig. 6C–E in Reig and Sanchez-Vives, 2007). For that reason, the stimulus-evoked synaptic potentials were sorted offline into those occurring during Down states and not evoking an Up state and those occurring during Up states (Fig. 1D,E). Auditory responses were evoked by seven different intensities (55, 61, 67, 72, 77, 82, and 85 dB), that were given at random (90–100 stimuli per intensity). At least 10 sound-evoked synaptic potentials were averaged for each of the intensities and part of the cycle (Up or Down state). Those cases in which a synaptic potential during the Down state induced an Up state (Reig and Sanchez-Vives, 2007) have not been illustrated here and were excluded from the analysis given that the amplitude of the evoked synaptic potential cannot be disentangled from the network recruitment. Figure 2A illustrates raw traces of four different intensities with PSPs occurring during either Up or Down states, the average PSP for each intensity being averaged in Figure 2B. The average PSP's amplitude for each intensity for

Down and Up states are represented for this particular neuron in Figure 2C.

For sound stimuli of intensities ranging between 55 and 85 dB, the average amplitudes of the evoked PSPs during Down states for the population ranged between 1 and 9 mV, the amplitude increasing with the stimulus intensity. However, those evoked by the same stimulus intensities during Up states varied within a narrower range of amplitudes: 4.3–6.5 mV. The stimulus–response relationship was thus attenuated during Up states with respect to Down states. Figure 2D shows a reduced stimulus–response relationship during Up states with respect to Down states. This is a representative example of the global scaling that takes place during Up states: for auditory stimuli and within these range of intensities, scaling occurs mostly as potentiation of small responses. The stimulus–response relationship, however, is maintained (Fig. 2C for an example of a single case), although reduced.

For lower intensities of stimulation (55 and 61 dB), the synaptic potentials evoked during Up states were significantly larger than those evoked during Down states ($p < 0.02$ for 55 dB and $p < 0.05$ for 61 dB; Fig. 2E). For louder stimuli ($\geq$67 dB), the difference between the amplitudes of synaptic potentials evoked in the Up and Down states disappeared. In some cases, for louder stimuli, we observed the inverted phenomenon; namely larger PSPs in Down than in Up states. This was the case, for example, in
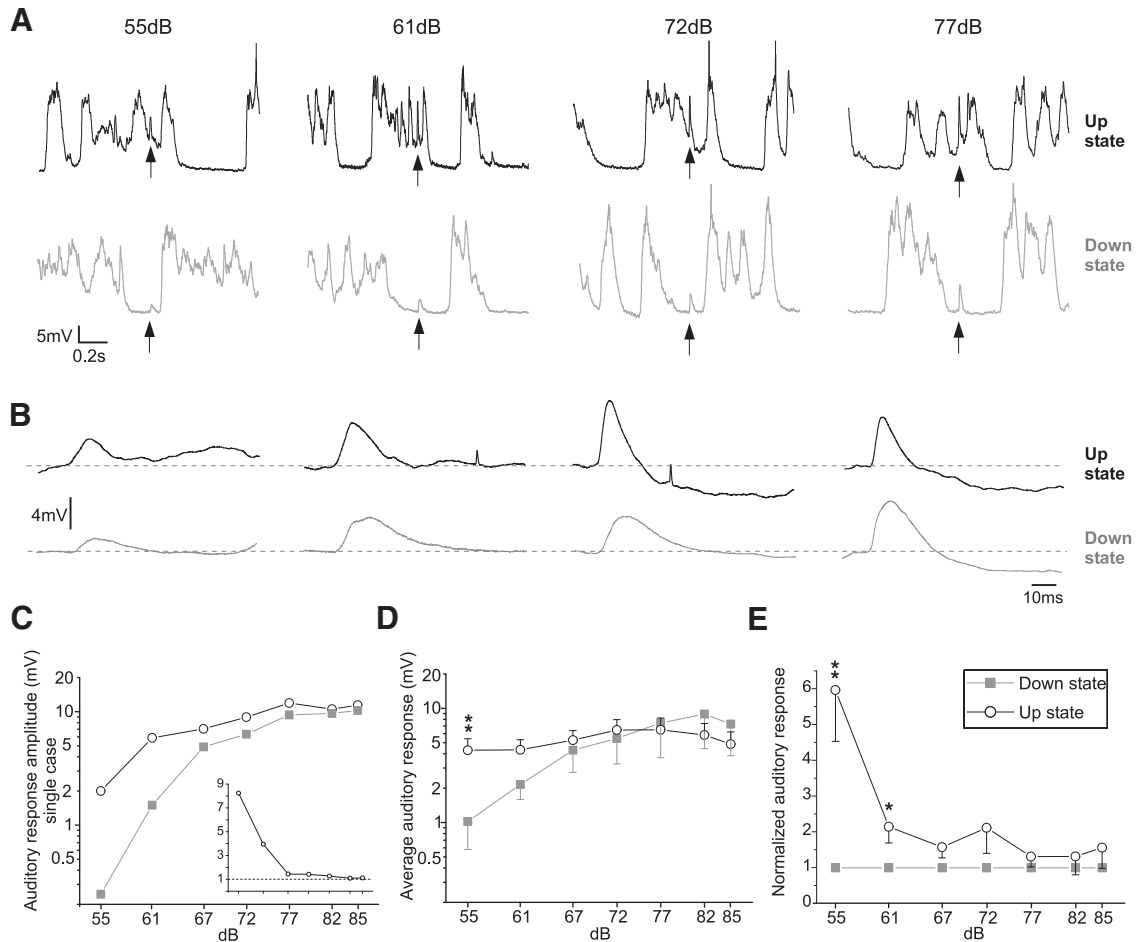
Figure 2. Synaptic potentials evoked by auditory stimulation during Up and Down states. **A**, Raw traces of intracellular recordings displaying synaptic responses in one neuron. Responses to different intensities of auditory stimulation (55, 61, 72, and 77 dB) during Up and Down states (top and bottom, respectively). The black arrows indicate the time of occurrence of the auditory stimuli. **B**, Waveform average of the synaptic potential evoked by the corresponding intensity (in **A**) during Up (top traces) and Down states (bottom traces). **C**, Amplitudes of the sound-evoked synaptic responses during Up and Down states against intensity of stimulation in the neuron illustrated in **A** and **B**. Inset shows the normalized values with respect to the Down state for this neuron. **D**, Average amplitude of auditory synaptic responses during Down and Up states for different stimulation intensities ($n = 9$ cells). **E**, Average of the cell-by-cell normalization of the PSP amplitudes with respect to the ones in the Down state. t test $*p < 0.05$; $**p < 0.02$; $***p < 0.01$.

the average in Figure 2B response to 77 dB. That trend is also apparent in the population average (Fig. 2D, 82–85 dB), although the difference was not significant.

In conclusion, cortical synaptic potentials evoked by auditory stimulation had larger amplitudes in Up than in Down states for low-intensity stimulations (<61 dB). For louder stimuli, no difference between the evoked potentials was found between the Up and Down states. Interestingly, the average intensity/response relationship observed during Down states was diminished during Up states, where a scaling of the auditory responses occurred.

Intracortical activation

Intracortical electrical stimulation of the intracellularly recorded neurons evoked synaptic potentials with an average onset latency of 2.89 ± 1.16 ms and a latency to the peak of 7.75 ± 2.54 ms ($n = 9$). The rank of amplitudes of the synaptic potentials evoked by different stimulus intensities (30–90 μA) in these connections was larger than for the sound-evoked and thalamocortical ones: 0.3–29 mV. We also observed larger excitatory amplitudes evoked by intracortical than by either sensory or thalamocortical activation. One reason could be that sensory and thalamocortical activations recruit larger feedforward inhibition than intracortical synapses (Gil and Amitai, 1996).

The experimental design was similar to the one used for auditory stimulation: at least six different intensities were used (30, 40, 50, 60, 70, and 90 μA) in different time periods of the oscillatory cycle. The amplitude of synaptic potentials evoked with stimuli of lower intensities (Fig. 3B–E; 30–40 μA) was significantly larger when occurring during Up than during Down states. For intensities between 50 and 70 μA, there was no significant difference between those occurring in Down versus Up states. However, when intensities were increased further, in this case to 90 μA, the relative amplitude of the normalized evoked potential during the Up state was significantly smaller than that during the Down state, thus inverting the trend (Fig. 3E).

As observed for auditory stimulation, intracortical synaptic potentials evoked during Up states showed a weaker dependence on the intensity of stimulation (ranging on average between 1.5 and 12.3 mV) than those evoked during Down states (ranging on average between 0.7 and 17.5 mV; Fig. 3D). For weak stimulation, the evoked potentials were 2.1 times larger in the Up than in the Down states, but for more intense stimuli, amplitudes were larger during Down states (1.4 times). This is again largely suggestive of the scaling effect that the active cortical network imposes over inputs.
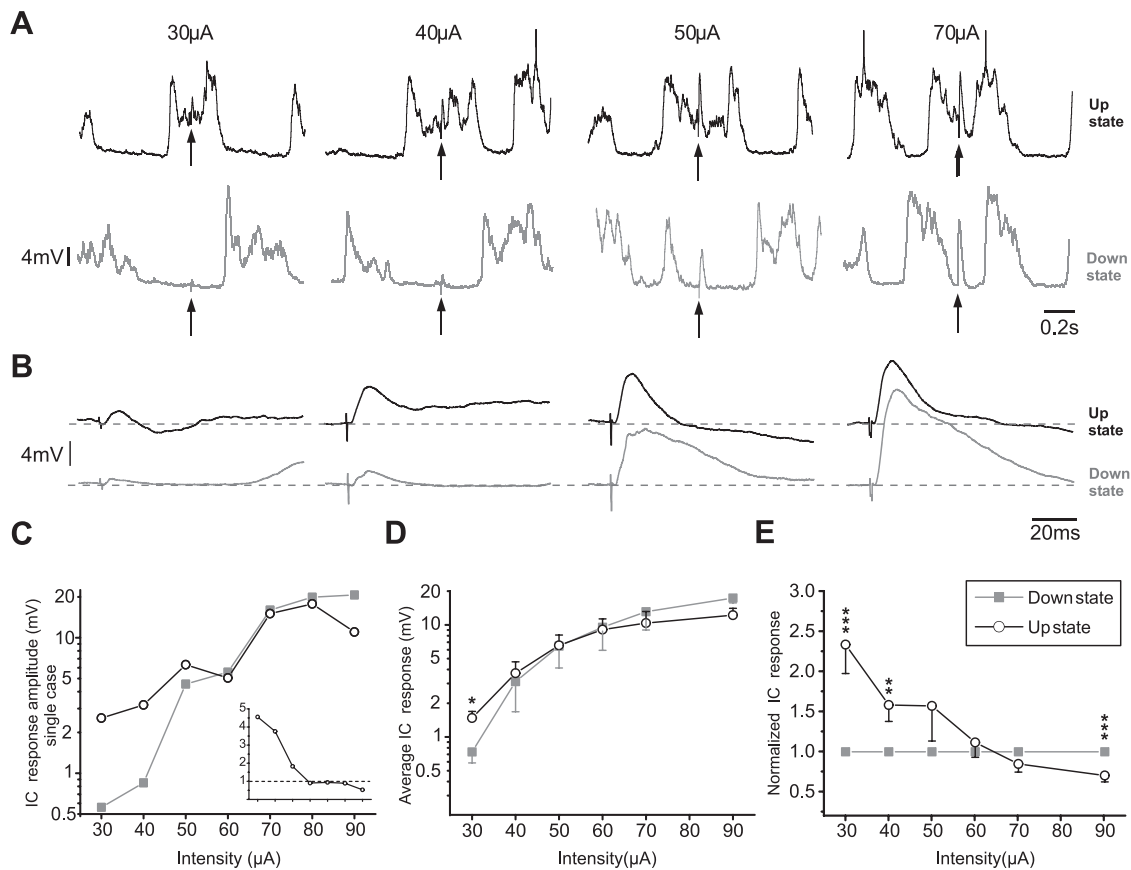
Figure 3. Synaptic potentials evoked by intracortical electrical stimulation during Up and Down states. *A*, Raw traces of intracellular recordings displaying synaptic responses in one neuron. Responses to different intensities of intracortical stimulation (30, 40, 50, 70 μA) during Up and Down states (top and bottom, respectively). The black arrows indicate the time of occurrence of the electrical stimuli. *B*, Waveform average of the synaptic potential evoked by the corresponding intensity (in *A*) during Up (top traces) and Down states (bottom traces). *C*, Amplitudes of the intracortically evoked synaptic responses during Up and Down states against intensity of stimulation in the neuron illustrated in *A* and *B*. In the inset, the normalized values with respect to the Down state for this neuron. *D*, Average amplitude of intracortical synaptic responses during Down and Up states for different stimulation intensities ($n = 9$ cells). *E*, Average of the cell-by-cell normalization of the PSP amplitudes with respect to the ones in the Down state. *t* test *$p < 0.05$; **$p < 0.02$; ***$p < 0.01$.

Thalamocortical activation

In this part of the study, postsynaptic potentials were evoked by means of electrical stimulation of the auditory thalamus ($n = 10$), their average onset latency being 3.85 ± 1.32 ms and a peak latency of 9.24 ± 1.58 ms. Four different stimulation intensities were tested (90, 120, 150, and 200 μA). Synaptic potentials evoked during both the Up and Down states had a significant stimulus–response relationship, their amplitudes increasing for larger intensities (Fig. 4*A*,*B*). A thalamic stimulus intensity of 90 μA evoked an average synaptic response of 1 mV during the Down state and 3.8 mV during the Up state. In general, for the three lower intensities (90, 120, and 150 μA), the synaptic potentials evoked during the Up states had in all cases significantly larger amplitudes than those occurring during Down states. However, synaptic potentials evoked by larger intensities (200 μA) were not significantly different in amplitude when evoked during Up versus during Down states (Fig. 4*D*,*E*). Similar to what we have described for sound-evoked potentials, the gain of synaptic potentials varied in the Up versus Down states and was stimulus dependent: weaker stimuli invariably evoked synaptic responses that were larger during Up states than those during Down states, the difference disappearing for stronger stimuli.

Modeling synaptic transmission during Up and Down states

Based on an idea introduced previously (Hô and Destexhe, 2000), we considered that the experimentally observed gain modulation could be understood as a result of the interaction between the

Up/Down variations in network excitability and input impedance. To test this possibility, we used the tools presented in the Model section of Materials and Methods to investigate the modulation predicted by artificial neural networks displaying either the Up state or the Down state activity. We illustrate this modulation on the effect of electrical stimulation of the cortical and the thalamic network consecutively. We derive the relationship between the current intensity value and the postsynaptic response in those two stimulation paradigms. The different steps that construct this relationship are detailed next.

Gain modulation in a cortical model: postsynaptic response to intracortical stimulation

We started by modeling the effect of the electrical stimulation. The bipolar stimulation in Figure 5*A* spreads over the local cortical network (the 1 mm circumference around the stimulation electrode where the recorded cell also lies). Each neuron within this network will be depolarized by the local extracellular current according to Equation 7. The extracellular field decays as stated by Equation 6 because of resistive dissipation, whereas the number of neurons reached raises with distance from the electrode (Equation 8). Those two factors lead to the histogram of induced depolarization across the cortical network (Equation 9) such that many distant neurons are weakly depolarized, whereas the few neurons close from the electrode are strongly depolarized. The histograms of activated neurons
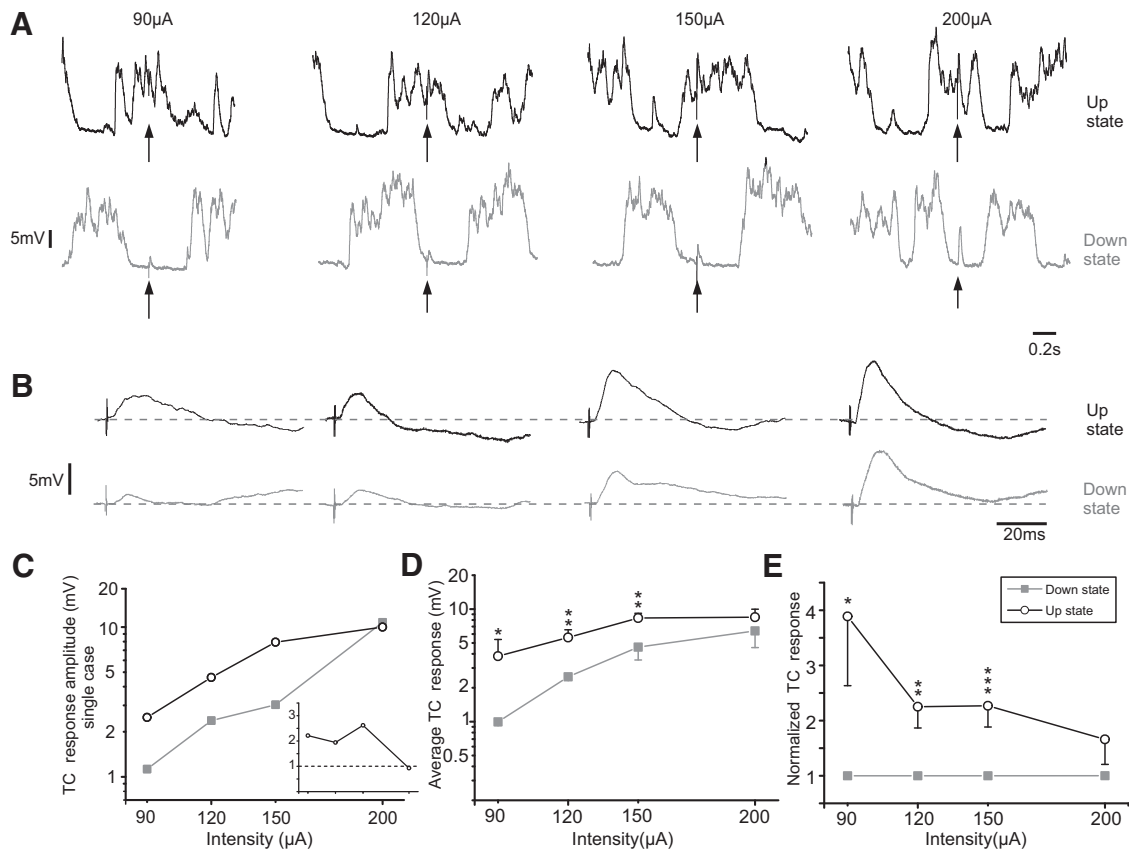
Figure 4. Synaptic potentials evoked by thalamocortical electrical stimulation during Up and Down states. ***A***, Raw traces of intracellular recordings displaying synaptic responses in one neuron. Responses to different intensities of thalamocortical stimulation (90, 120, 150, 200 μA) during Up and Down states (top and bottom, respectively). The black arrows indicate the time of occurrence of the electrical stimuli. ***B***, Waveform average of the synaptic potential evoked by the corresponding intensity (in ***A***) during Up (top traces) and Down states (bottom traces). ***C***, Amplitudes of the thalamocortically evoked synaptic responses during Up and Down states against intensity of stimulation in the neuron illustrated in ***A*** and ***B***. In the inset, the normalized values with respect to the Down state for this neuron. ***D***, Average amplitude of thalamocortical synaptic responses during Down and Up states for different stimulation intensities ($n = 10$ cells). ***E***, Average of the cell-by-cell normalization of the PSP amplitudes with respect to the ones in the Down state. t test $*p < 0.05$; $**p < 0.02$; $***p < 0.01$.

for three different levels of injected current I are represented in Figure 5B.

The cortical network translates this stimulation into different firing intensities for the two different network states. In the Up state, the background activity amplifies the effect of the stimulation. The evoked depolarization brings many neurons to suprathreshold levels and evokes firing because of membrane potential fluctuations and initial depolarization (Nowak et al., 1997). This is not the case in the Down state, where only the few neurons depolarized above threshold by the stimulus reach the threshold and fire. Following the method of Hô and Destexhe (2000), we introduce the "activation function" of the network that translates the stimulus value into the probability to evoke a spike. This can be calculated explicitly from the fluctuations of the membrane potential and a basic threshold mechanism for spiking (Equation 11). The comparison of the functions between Up and Down states is illustrated in Figure 5C. The activation function is convoluted with the histogram of depolarization to obtain the number of activated neurons (Equation 12). Note that in the Up state, this "activation function" should be applied only to the neurons that would be silent in the absence of stimulation. To calculate the number of cells responding to the evoked input, we first discard the fraction of the network that participates in the baseline firing rate and therefore to the baseline conductance and depolarization levels (see Materials and Methods). An example of this procedure is presented in Figure 5D for a stimulus current of

60 μA. We show the distribution of "available" neurons, (those that do not participate in the baseline rate), and we convolute this distribution with the activation function, to get the number of activated neurons (the shaded parts of the histogram). We repeat this procedure for all stimulation levels and count the total number of activated neurons within the cortical network, leading to the plot in Figure 5E. Therefore, for every stimulation level I, we have a number of activated neurons $N_{act}(I)$. To obtain the postsynaptic response, we first calculated the number of afferent activated neurons onto the recorded cell. Given a random recurrent connectivity $\varepsilon_{cort} = 2\%$ (the connectivity of the network is considered homogeneous within the defined local cortical network) and a fraction of inhibitory neurons $g = 25\%$, the recorded neuron will have $N_e = N_{act}(I) \cdot (1 - g)$ and $N_i = N_{act}(I) \cdot g$ excitatory and inhibitory active synapses, respectively. The maximum depolarization value induced by this stimulation is then given by calculating the time of maximum amplitude (Equation 17) and evaluating the membrane potential time course (Equation 16) at that time. The synaptic and membrane parameters used in this calculation can be found in Table 1. The whole procedure results in Figure 5, *F* and *G*, where the postsynaptic response and the modulation factor for evoked intracortical postsynaptic potentials in Up versus Down states are represented. The gain modulation imposed by the Up and Down states results in a scaling of the responses, potentiating the smaller responses and dampening
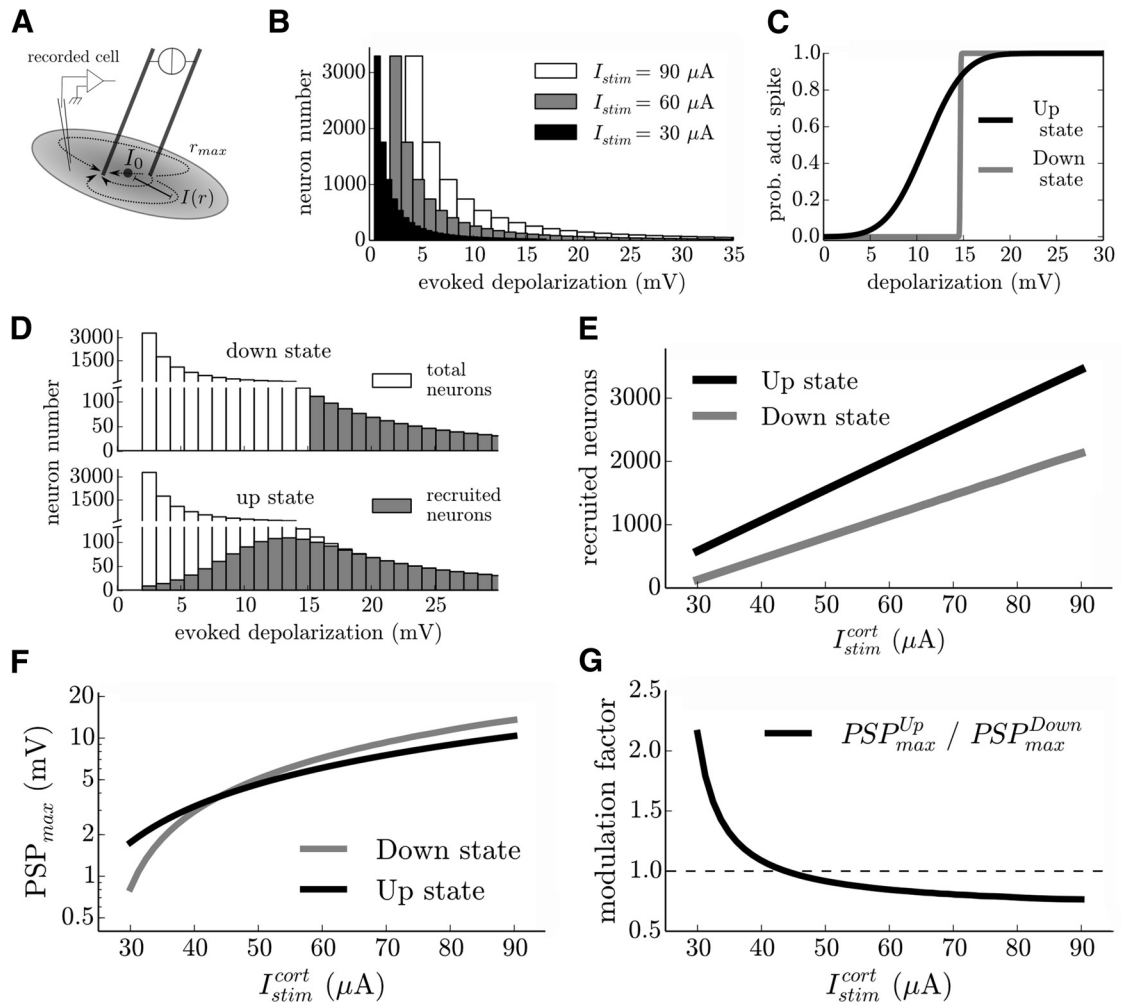
Figure 5. Modeling the effect of intracortical electrical stimulation on cortical postsynaptic potentials. **A**, We define a local cortical network that is sensitive to the stimulation; the recorded cell is part of it and receives recurrent input from this network. **B**, Recruitment of neurons for different stimulation intensities. Stimulation $N_I(\Delta V)$ (Equation 16) of the local cortical network given the decaying stimulus intensity $I(r)$ and the increasing cell density $N(r)$. **C**, The activation function represents the excitability of the cortical network. It estimates the probability to elicit a spike as a response to the stimulation (for the cell's fraction that does not participate in the background activity level in the considered time bin, see Materials and Methods) **D**, The number of recruited neurons by the IC stimulation is the convolution of the depolarization histogram with the activation function. We show for $I = 80$ μA how the recruitment differs between Up and Down states. **E**, Repeating the procedure of **D** for all intensity levels provides the number of activated neurons within the network as a function of the current stimulation. **F**, For given network parameters, we can estimate the network input to the recorded cell and deduce the maximum postsynaptic potential to be compared with the experimental results of Figure 2C. **G**, Modulation factor (amplitude of PSP in Up state divided by amplitude of PSP in Down state) as a function of the stimulus intensity.

the larger ones in a similar way to the experimental intracortical stimulation (Figs. 3E, 7).

Gain modulation in a thalamocortical model: cortical postsynaptic response to thalamic stimulation

We investigated the impact of the thalamic processing of the input on the gain modulation. To that end, we included the change of the excitability properties of the thalamic network between Up and Down states. Indeed, the *in vivo* intracellular study of (Contreras et al., 1996) shows that the Up state has an impact in the thalamic neurons (membrane depolarization and conductance increase). Therefore, the recruitment effect that we described for the intracortical stimulation case (see above) applies not only for the cortical, but also for the thalamic network. We implemented this idea in a model, simplifying the thalamocortical model presented in Destexhe (2009) to adapt it to our situation (see Materials and Methods). To construct the current-depolarization relationship, we first model the TC stimulation that recruits thalamic neurons in a state-dependent manner (Fig. 6B, shown for $I^{thal} = 145$ μA) following their different

activation function (Fig. 6A). This results in a mean number of activated TC neurons $N_{act}^{thal}(I^{thal})$ as a function of the injected current. We hypothesize a random projection between the thalamic network of size $N_{tot}^{thal} = 2000$ and the cortical network of size $N_{tot}^{cort} = 10000$ with a probability $\varepsilon^{thal} = 2\%$. The number of activated synapses onto cortical neurons will result from the sampling of $N_{act}^{cort}(I^{thal})$ neurons with a connection probability ε^{thal}, which means that the number of activated synapses over the cortical network will follow a binomial distribution (Fig. 6C, shown for $I^{thal} = 145$ μA). With the parameters of the thalamocortical synapse (Table 1), we translate a number of activated excitatory synapses into a maximum depolarization using Equation 17 (expression for the time of maximum amplitude) and Equation 16 (time course of the membrane potential variations). In this way, we generate a histogram of depolarization over the available neurons on which we can apply the activation function (Fig. 6D, shown for $I^{thal} = 145$ μA) to get the number of activated neurons in the cortical network $N_{act}^{cort}(I^{thal})$. In Figure 6E, we show the number of activated TC neurons (inset) and cortical neurons
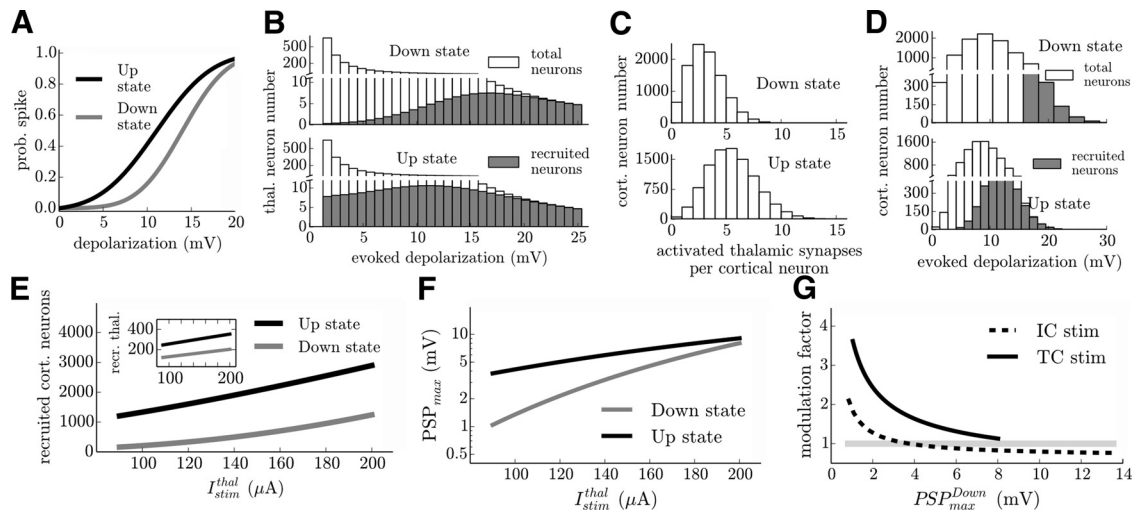
Figure 6. Modeling the effect of thalamocortical electrical stimulation on cortical postsynaptic potentials. **A**, Activation functions of the thalamic cells that represent the difference of excitability of the thalamic network in the Up and Down states, respectively. **B**, The recruitment within the thalamic network is done as in the cortical case (see Fig. 4). The procedure allows to have a number of activated thalamic cells in the Up and Down states, shown for $I_{stim}^{thal} = 145 \ \mu A$. **C**, Histogram over the cortical network (binomial distribution) of the number of activated afferent TC synapses per cortical neuron, shown for the same level of stimulation. **D**, Each number of activated synapses can be translated into a depolarization level. This provides the histogram of the depolarization over the cortical network. The number of activated cortical neurons is calculated (as in the IC stimulation case) by convolution of the depolarization histogram with the activation function. **E**, We repeat this procedure for all levels of the TC stimulation levels and get the number of activated TC cells (inset) and the number of activated cortical cells as a function of the stimulation level in the Up and Down states, respectively. **F**, Amplitude of PSP as a function of the current stimulation level. **G**, Modulation factor as a function of the PSP amplitude in the Down state. Shown is a comparison between the model of IC stimulation and TC stimulation. The gain modulation between Up and Down state is greatly increased with respect to the cortical case as a consequence of the cumulative effect of the increased excitability of the cortical and thalamic networks.

(main plot) for all values of stimulation intensities. Finally, as in the previous section, we calculate the mean postsynaptic response resulting from the activation of those $N_{act}^{cort}(I^{thal})$. This is shown in Figure 6F for a whole range of stimulus intensities.

Comparing the modulation in the different stimulation types
In the models, we get an equal postsynaptic response of 2 mV in the Down state for $I^{thal} = 116.9 \ \mu A$ and for $I^{cort} = 36.1 \ \mu A$. In the Up state, this stimulation intensity corresponds to two different postsynaptic responses: 2.6 and 4.9 mV for the IC and TC stimulation, respectively. Because the cortical network has the same activation function in the two situations, the origin of this potentiation in the TC case comes from the enhanced excitability of the thalamic network in the Up state (as can be seen in the activation function; Fig. 6A). Indeed, in this model, only two phenomena can lead to a difference between the IC and TC stimulation cases: the enhanced excitability of the thalamic network and the scaling of the thalamocortical postsynaptic effect on cortical cells because of the conductance state of the cortical cells. The first one potentiates the Up state response and the second one attenuates it. We found that, for our parameters, the combination of those two effects is in favor of the Up state potentiated response. We plot in Figure 6G the modulation as a function of the Down state response in the IC and TC cases. The deviation between the two curves is the trace of the modulation that happens in the thalamic nucleus.

To compare with the experimental data in Figure 7, we represented the modulation factor of postsynaptic responses as a function of the Down state for both IC and TC stimulation. As predicted by the model (Fig. 6G), the increase in the modulation in the TC case with respect to the IC is evident, as is the scaling of the postsynaptic responses. The introduced model provides a feasible mechanistic explanation for this experimental observation.
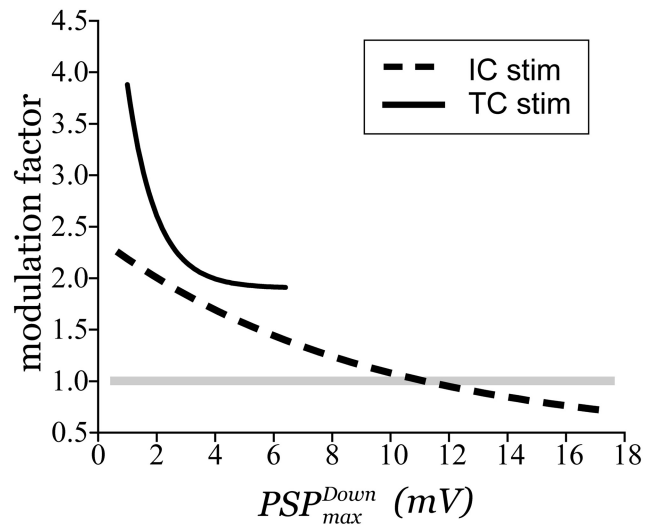

Figure 7. Experimental modulation factor for TC and IC synaptic inputs. Comparison of the input modulation factor as a function of the Down state response for TC and IC stimuli. The TC stimulation paradigm displayed a larger modulation than the IC stimulation. Auditory and TC stimulation involve the thalamocortical pathway while the IC stimulation only involves the recurrent cortical network. A mechanism such as the one discussed in the text and illustrated in Figure 5 could explain this increased modulation by taking into account the impact of both the thalamic and cortical network excitability in the Up state.

Discussion

Cortical dynamics during Up states are similar in various aspects to those during cortical activated states or wakefulness (for a review, see Destexhe et al., 2007). That is one reason why the study of synaptic responsiveness during Up and Down states is relevant for understanding information transmission and processing in different brain states, in particular during wakefulness. In this study, we have recorded Up and Down states in the auditory cortex. In different cortical areas, the transition from anes-

thesia or deep sleep to awake has been described as an elongation or persistence of the Up states (Steriade et al., 2001; Constantinople and Bruno, 2011). Even when slow oscillatory activity has been also studied by others in the auditory cortex under anesthesia (Sakata and Harris, 2009), Hromádka et al. (2013) reported that Up states are rare in the awake auditory cortex. The possibility exists that auditory cortex would be a special case on this regard. However, it is known that the dynamics of the network slow oscillatory activity are very sensitive to the brain state. In a study by Deco et al. (2009), the emergent activity in both deep and light anesthesia is described in auditory cortex. There, when in light anesthesia, the silent state is more depolarized and the dynamics of Down/Up transitions are radically different from those in deep anesthesia, the membrane potential remaining for longer periods in depolarized values. Furthermore, the content of high frequencies during silent states is larger in light than in deep anesthesia. In Figure 5 of Hromádka et al. (2013), the silent state also shows both more depolarized values and larger high-frequency activity in the awake than under anesthesia. Based on this, one could argue that in the awake auditory cortex the silent state does not exactly correspond to a "classical" Down state.

The influence that Up states have on sensory or synaptic transmission has been studied in different systems (see Introduction). However, there is no consensus as to whether synaptic transmission during cortical Up states is increased or decreased with respect to Down states (see below). In the study that we present here, we have evoked synaptic potentials in primary auditory cortex *in vivo* by three means: auditory stimulation and intracortical and thalamocortical electrical stimulation with stimuli of different intensities. Synaptic potentials evoked during Up states were compared with those evoked during Down states with the same stimulus intensity. For all types of stimulation, we found that the relative synaptic transmission in Up versus Down states is critically dependent on the intensity of stimulation. Our results show that, during Up states, there is gain modulation of synaptic responses such that the transmission of small inputs is potentiated and very strong inputs are attenuated, resulting in a scaling of the responses. This was the case for all forms of stimulation and it was especially evident for intracortical stimulation.

Synaptic transmission in Up versus Down states: increased or decreased?

The issue of how Up states and therefore network activity affects synaptic inputs has been discussed by different investigators. Studies in the visual cortex generally found increased responses during Up states, both suprathreshold and subthreshold (Arieli et al., 1996; Azouz and Gray, 1999; Haider et al., 2007; Reig and Sanchez-Vives, 2007). However, several studies in barrel cortex reported that, during Up states, responsiveness was decreased with respect to that during Down states (Castro-Alamancos and Oldford, 2002; Sachdev et al., 2004; Crochet et al., 2006; Hasenstaub et al., 2007; Rigas and Castro-Alamancos, 2009).

An increase in responsiveness during Up states is quite straightforward to explain: during these periods, the excitability of the thalamocortical network is increased and thus any stimulus recruits more presynaptic inputs. Postsynaptically, neurons are depolarized and are thus closer to threshold during Up states and are therefore more responsive to inputs. These arguments have been used to explain increased responsiveness in visual cortex (Arieli et al., 1996; Azouz and Gray, 1999; Haider et al., 2007; Reig and Sanchez-Vives, 2007).

Different mechanisms can also be invoked to explain the opposite, why synaptic responses may decrease during Up versus Down states. That both thalamocortical and intracortical synaptic responses depress with activity has been used as an argument supporting why synaptic transmission is attenuated during Up states (Castro-Alamancos and Oldford, 2002). A smaller driving force for glutamatergic transmission during Up states (Castro-Alamancos, 2002; Petersen et al., 2003; Sachdev et al., 2004), increased membrane conductance (Hasenstaub et al., 2007), an increase in the action potential threshold (Sachdev et al., 2004), or low calcium during Up states (Crochet et al., 2005), are among the other possible mechanisms that might override the increased excitability during Up states.

Differences in intrinsic properties across cortical areas could contribute to differences across areas. For example, the apparent input resistance in Up states appears to be very low in cat association cortex (Paré et al., 1998) but high in rat barrel cortex (Zou et al., 2005; Waters and Helmchen, 2006). Our conductance measurements in auditory cortical neurons reported above find a 1.3–3.3 times larger conductance in Up than in Down states in regular spiking neurons, probably due to the accumulation of excitatory and inhibitory synaptic events described in A1 during Up states (Compte et al., 2009). Such differences in input resistance may also contribute to the observed differences of responsiveness, which further emphasizes the need to precisely measure the conductance state in Up/Down states.

Despite the different mechanisms just mentioned, we propose here two possible explanations supporting the disparate results reported so far in the literature about cortical activation and its effects on responsiveness. One is the relevance of the stimulation intensity because we find that, in the same system (auditory, in the present study), one can observe both increases and decreases of the synaptic response depending on the stimulus intensity. Therefore, different intensities of stimulation used by different groups could generate different results.

Another critical element is the degree of network recruitment integrated in the synaptic response evoked during Down states that is taken as a reference. Given that synaptic responses during Up states are evaluated against those during Down states, the measurements of synaptic responses during Down states is crucial. Synaptic potentials occurring during Down states can trigger or not a new Up state. The probability to induce an Up state is larger for larger-intensity stimuli. When a synaptic response is large enough to recruit the local network and activate an Up state, the evoked synaptic amplitude includes the postsynaptic potential plus the reverberation of activity in the network (Fig. 6 in Reig and Sanchez-Vives, 2007). To correctly compare synaptic responses in Down versus Up states, it is critical to include only synaptic responses in Down states, and not the evoked synaptic reverberation. When the intensity of stimulation is large but not maximum, the synaptic potential occurring during the Down state is immediately followed by an Up state (Reig and Sanchez-Vives, 2007). In these cases, the amplitude of the synaptic potential is still well segregated in time from that of the Up state and can be measured separately. For still larger intensities, the network recruitment by the stimulus is immediate and therefore the network activation cannot be separated from the synaptic potential. In some of the studies discussed above, the stimulation was such that the responses during Down states always included the network response. This can result in a mistaken detection of a large synaptic response during Down states such that the one during Up states appears decreased in comparison.

In the present study, we only included stimulus intensities that did not trigger an Up state. This limits the use of high-intensity stimuli. This was the case for auditory and thalamocortical stim-

ulation, whereas intracortical stimuli could be of large amplitudes without recruiting Up states. This is probably why intracortical stimuli was the one where an actual decrease of the synaptic potential amplitudes during Up states was more obvious for high-intensity stimuli. When the intensity of stimulation is low, this problem does not arise because Up states are not recruited by the stimulation. For low-intensity stimulation, the responses during Up states were invariably increased with respect to those during Down states (Figs. 2, 3, 4). This increment was independent of how the synaptic potential was evoked (auditory, intracortical, or thalamocortical stimulation).

Scaling of synaptic inputs during Up states

The effect of network state that we have described here results in gain modulation of the incoming inputs, enhancing small inputs and attenuating very large ones while still maintaining the intensity–response relationship. This change in the input/output slope during activated states of the cortex could have a function expanding the range of inputs that can be processed, improving detectability of weak inputs.

The model that we introduce here provides a possible mechanism to explain the experimentally observed properties. We find that Up and Down states represent different modes of treatment of the synaptic input: the first uses the depolarization and the fluctuations to amplify the input at the network level and the latter makes use of a low conductance state to generate strong postsynaptic responses.

To explain the results of thalamocortical inputs, we had to consider a double gain modulation in both thalamic cells (Wolfart et al., 2005) and cortical recipient cells. Our model shows that the combined action of synaptic noise on these two interconnected networks can lead to a duplication of the gain modulation effects on synaptic responsiveness. The feedforward arrangement of excitable neural networks is a powerful mechanism to enhance the propagation of the Up state response compared with the Down state response. It also suggests that such combined effects may need to be taken into account for interpreting responses in areas downstream to A1, which should be investigated in future studies. Furthermore, our model results suggest the need of precise measurements of synaptic noise in different areas to correctly reconstruct the combined effect of integrating information from different networks.

References

Arieli A, Sterkin A, Grinvald A, Aertsen A (1996) Dynamics of ongoing activity: explanation of the large variability in evoked cortical responses. Science 273:1868–1871. CrossRef Medline

Azouz R, Gray CM (1999) Cellular mechanisms contributing to response variability of cortical neurons in vivo. J Neurosci 19:2209–2223. Medline

Boudreau CE, Ferster D (2005) Short-term depression in thalamocortical synapses of cat primary visual cortex. J Neurosci 25:7179–7190. CrossRef Medline

Castro-Alamancos MA (2002) Different temporal processing of sensory inputs in the rat thalamus during quiescent and information processing states in vivo. J Physiol 539:567–578. CrossRef Medline

Castro-Alamancos MA, Oldford E (2002) Cortical sensory suppression during arousal is due to the activity-dependent depression of thalamocortical synapses. J Physiol 541:319–331. CrossRef Medline

Compte A, Reig R, Sanchez-Vives M (2009) Timing excitation and inhibition in the cortical network. In: Coherent behavior in neuronal networks (Josic K, Rubin J, Matias M, Romo R, eds), pp 17–46. New York: Springer.

Constantinople CM, Bruno RM (2011) Effects and mechanisms of wakefulness on local cortical networks. Neuron 69:1061–1068. CrossRef Medline

Contreras D, Timofeev I, Steriade M (1996) Mechanisms of long-lasting hyperpolarizations underlying slow sleep oscillations in cat corticothalamic networks. J Physiol 494:251–264. CrossRef Medline

Cowan RL, Wilson CJ (1994) Spontaneous firing patterns and axonal projections of single corticostriatal neurons in the rat medial agranular cortex. J Neurophysiol 71:17–32. Medline

Crochet S, Chauvette S, Boucetta S, Timofeev I (2005) Modulation of synaptic transmission in neocortex by network activities. Eur J Neurosci 21:1030–1044. CrossRef Medline

Crochet S, Fuentealba P, Cissé Y, Timofeev I, Steriade M (2006) Synaptic plasticity in local cortical network in vivo and its modulation by the level of neuronal activity. Cereb Cortex 16:618–631. Medline

Deco G, Martí D, Ledberg A, Reig R, Vives MVS (2009) Effective reduced diffusion-models: a data driven approach to the analysis of neuronal dynamics. PLoS Comput Biol 5:e1000587. CrossRef Medline

Destexhe A (2009) Self-sustained asynchronous irregular states and Up-Down states in thalamic, cortical and thalamocortical networks of nonlinear integrate-and-fire neurons. J Comput Neurosci 27:493–506. CrossRef Medline

Destexhe A, Contreras D (2006) Neuronal computations with stochastic network states. Science 314:85–90. CrossRef Medline

Destexhe A, Hughes SW, Rudolph M, Crunelli V (2007) Are corticothalamic 'up' states fragments of wakefulness? Trends Neurosci 30:334–342. CrossRef Medline

Gil Z, Amitai Y (1996) Properties of convergent thalamocortical and intracortical synaptic potentials in single neurons of neocortex. J Neurosci 16:6567–6578. Medline

Haider B, Duque A, Hasenstaub AR, Yu Y, McCormick DA (2007) Enhancement of visual responsiveness by spontaneous local network activity in vivo. J Neurophysiol 97:4186–4202. CrossRef Medline

Hasenstaub A, Sachdev RN, McCormick DA (2007) State changes rapidly modulate cortical neuronal responsiveness. J Neurosci 27:9607–9622. CrossRef Medline

Hô N, Destexhe A (2000) Synaptic background activity enhances the responsiveness of neocortical pyramidal neurons. J Neurophysiol 84:1488–1496. Medline

Hromádka T, Zador AM, DeWeese MR (2013) Up states are rare in awake auditory cortex. J Neurophysiol 109:1989–1995. CrossRef Medline

Kuhn A, Aertsen A, Rotter S (2004) Neuronal integration of synaptic input in the fluctuation-driven regime. J Neurosci 24:2345–2356. Medline

Lapicque L (1907) Recherches quantitatives sur l'excitation électrique des nerfs traitée comme une polarisation. J Physiol Pathol Gen 9:620–635.

Logothetis NK, Kayser C, Oeltermann A (2007) In vivo measurement of cortical impedance spectrum in monkeys: implications for signal propagation. Neuron 55:809–823. CrossRef Medline

Lorente de No R (1938) Analysis of the activity of the chains of internuncial neurons. J Neurophysiol 1:207–244.

Luczak A, Barthó P, Harris KD (2009) Spontaneous events outline the realm of possible sensory responses in neocortical populations. Neuron 62:413–425. CrossRef Medline

Metherate R, Ashe JH (1993) Ionic flux contributions to neocortical slow waves and nucleus basalis-mediated activation: whole-cell recordings in vivo. J Neurosci 13:5312–5323. Medline

Nowak LG, Sanchez-Vives MV, McCormick DA (1997) Influence of low and high frequency inputs on spike timing in visual cortical neurons. Cereb Cortex 7:487–501. CrossRef Medline

Nowak LG, Azouz R, Sanchez-Vives MV, Gray CM, McCormick DA (2003) Electrophysiological classes of cat primary visual cortical neurons in vivo as revealed by quantitative analyses. J Neurophysiol 89:1541–1566. Medline

Paré D, Shink E, Gaudreau H, Destexhe A, Lang EJ (1998) Impact of spontaneous synaptic activity on the resting properties of cat neocortical pyramidal neurons in vivo. J Neurophysiol 79:1450–1460. Medline

Paxinos G, Watson C (2005) The rat brain in stereotaxic coordinates, ed 5. Amsterdam: Elsevier Academic.

Petersen CC, Hahn TT, Mehta M, Grinvald A, Sakmann B (2003) Interaction of sensory responses with spontaneous depolarization in layer 2/3 barrel cortex. Proc Natl Acad Sci U S A 100:13638–13643. CrossRef Medline

Ranck JB Jr (1975) Which elements are excited in electrical stimulation of mammalian central nervous system: a review. Brain Res 98:417–440. CrossRef Medline

Rees A, Sarbaz A, Malmierca MS, Le Beau FE (1997) Regularity of firing of neurons in the inferior colliculus. J Neurophysiol 77:2945–2965. Medline

Reig R, Sanchez-Vives MV (2007) Synaptic transmission and plasticity in an active cortical network. PLoS One 2:e670. CrossRef Medline

Reig R, Gallego R, Nowak LG, Sanchez-Vives MV (2006) Impact of cortical network activity on short-term synaptic depression. Cereb Cortex 16:688–695. CrossRef Medline

Richardson MJ (2004) Effects of synaptic conductance on the voltage distribution and firing rate of spiking neurons. Phys Rev E Stat Nonlin Soft Matter Phys 69:051918. CrossRef Medline

Rigas P, Castro-Alamancos MA (2009) Impact of persistent cortical activity (up States) on intracortical and thalamocortical synaptic inputs. J Neurophysiol 102:119–131. CrossRef Medline

Rudolph M, Piwkowska Z, Badoual M, Bal T, Destexhe A (2004) A method to estimate synaptic conductances from membrane potential fluctuations. J Neurophysiol 91:2884–2896. CrossRef Medline

Sachdev RN, Ebner FF, Wilson CJ (2004) Effect of subthreshold up and down states on the whisker-evoked response in somatosensory cortex. J Neurophysiol 92:3511–3521. CrossRef Medline

Sakata S, Harris KD (2009) Laminar structure of spontaneous and sensory-evoked population activity in auditory cortex. Neuron 64:404–418. CrossRef Medline

Sanchez-Vives MV, McCormick DA (2000) Cellular and network mechanisms of rhythmic recurrent activity in neocortex. Nat Neurosci 3:1027–1034. CrossRef Medline

Sanchez-Vives MV, Nowak LG, Descalzo VF, Garcia-Velasco JV, Gallego R, Berbel P (2006) Crossmodal audio-visual interactions in the primary visual cortex of the visually deprived cat: a physiological and anatomical study. Prog Brain Res 155:287–311. CrossRef Medline

Seamari Y, Narváez JA, Vico FJ, Lobo D, Sanchez-Vives MV (2007) Robust off- and online separation of intracellularly recorded up and down cortical states. PLoS One 2:e888. CrossRef Medline

Steriade M (2001) Impact of network activities on neuronal properties in corticothalamic systems. J Neurophysiol 86:1–39. Medline

Steriade M, Nuñez A, Amzica F (1993) A novel slow (<1 Hz) oscillation of neocortical neurons in vivo: depolarizing and hyperpolarizing components. J Neurosci 13:3252–3265. Medline

Steriade M, Timofeev I, Grenier F (2001) Natural waking and sleep states: a view from inside neocortical neurons. J Neurophysiol 85:1969–1985. Medline

Timofeev I, Contreras D, Steriade M (1996) Synaptic responsiveness of cortical and thalamic neurones during various phases of slow sleep oscillation in cat. J Physiol 494:265–278. CrossRef Medline

Waters J, Helmchen F (2006) Background synaptic activity is sparse in neocortex. J Neurosci 26:8267–8277. CrossRef Medline

Wolfart J, Debay D, Le Masson G, Destexhe A, Bal T (2005) Synaptic background activity controls spike transfer from thalamus to cortex. Nat Neurosci 8:1760–1767. CrossRef Medline

Zou Q, Rudolph M, Roy N, Sanchez-Vives M, Contreras D, Destexhe A (2005) Reconstructing synaptic background activity from conductance measurements in vivo. Neurocomputing 65:673–678. CrossRef